Progress In Electromagnetics Research Letters, Vol. 73, 17–22, 2018

A Broadband Low-Loss WR 10 Waveguide to Microstrip Line Transition with T-Shaped Probe

Gerhard F. Hamberger*, Uwe Siart, and Thomas F. Eibert

Abstract—A novel W-band WR 10 waveguide to microstrip line transition is designed, simulated in a 3D full-wave EM simulation software, fabricated, and evaluated by measurements. The main advantages of this transition are frequency-flat transmission, low reflection, and uncomplicated fabrication. Simulation shows a reflection coefficient of better than −23 dB from 75 to 90 GHz for one hollow waveguide to microstrip line transition. The port reflections increase for a fabricted prototype with two transitions and a connecting microstrip line to a level of about −14 dB. This is mainly caused by fabrication tolerances. The overall transmission of the dual transition prototype is found at a very satisfactory level of about −4.8 dB at 90 GHz for a connecting microstrip line with a length of 45 mm corresponding to an estimated loss of approximately 0.6 dB for a single transition.

1. INTRODUCTION

Millimeter-wave frequencies have been attracting increasing attention in mass market and consumer applications over the past years. Especially communication systems but also radar applications are heading towards frequency bands in the mm-wave region to enhance the available bandwidth. The frequency band around 28 GHz is a hot candidate for the fifth generation of mobile cellular communication. From 57 to 64 GHz [1], there is a designated band for wireless point-to-point links and the band from 76 to 81 GHz is used for automotive radar applications.

Especially in the W-band, precise measurement of components and systems is very difficult due to the short wavelengths. Even though there are coaxial connectors covering the frequency range up to 110 GHz, the cable losses are much higher compared to those of rectangular hollow waveguides (WGs). Most commercial W-band vector network analyzers use external multiplier modules with WR 10 WG ports to connect the device under test.

Automotive radar front-ends are reasonably fabricated on planar high-frequency substrates, because of low cost and low weight. For the measurement of radiating structures, a transition from WG to microstrip line is necessary, which can be implemented by many different methods. An antipodal finline is used to connect the substrate longitudinally to the WG in [2], but it is very difficult to reliably connect the substrate structure to the WG walls. The WG can also be mounted orthogonal to the substrate, comparable to [3–5]. Seo summarized different transitions in [6] and proposed a vertical interconnect access (VIA) less transition in [7]. All the concepts are either WG back-ended stub based or use direct coupling with a structure element (slot or patch) on the WG mounting side of the substrate. The slot or patch couples directly to the microstrip line which is inset into the waveguide short. W-band frequencies require small gaps between microstrip line and waveguide short of approx. 100 µm which are hard to fabricate reliably. The VIA less transition has one main drawback. The parallel plate substrate mode

Received 11 August 2017, Accepted 10 November 2017, Scheduled 23 January 2018

* Corresponding author: Gerhard F. Hamberger (gerhard.hamberger@tum.de).

The authors are with the Chair of High-Frequency Engineering, Department of Electrical and Computer Engineering, Technical University of Munich, Germany.

is excited, and some power is radiated by the transition. Obviously, such transitions are not preferable for the measurement of radiating structures like antennas.

A transition with a back-ended stub and a T-shaped E-field probe for highest transmission and very good port matching is proposed in this paper. The theoretical background is described in Section 2. Section 3 shows the simulation model of the transition and Section 4 includes simulation and measurement results of a double-transition prototype, especially designed for measurement purposes.

2. DESIGN CONSIDERATIONS

The operating frequency range of a WG is bounded below by the cutoff frequency of the fundamental mode and at above by the cutoff frequency of the first higher-order mode. Due to the boundary conditions of the WG, transversal-electric (TE_{mn}) and transversal-magnetic (TM_{mn}) waves can exist in the waveguide, where m and n indicate the mode orders. Either electric or magnetic field components are zero for TM modes if m or n equals zero, so that the lower modes of a WG are TE modes [8]. The cutoff frequency of the TE_{mn} mode is defined by the geometry of the WG. Through the chosen aspect ratio of $\frac{a}{b} = \frac{2}{1}$ for most standardized WGs, the relative bandwidth of the commonly used fundamental TE_{10} mode is 50%, since the next higher order mode is the TE_{20} mode [9]. The transition is designed for the frequency range from 75 to 81 GHz, where a dual-polarized antenna array is fed from WGs [10]. In this frequency range, two standardized WGs can be used, WR 10 and WR 12. The proposed transition is based on a WR 10 waveguide with smaller geometric dimensions.

A main part of this transition is a WG short circuit in the WR 10 waveguide. The conducting material, used as WG boundary and short, forces the tangential E-field to be 0. The next E-field maximum, seen from the short, is found $\frac{\lambda_\mathrm{g}}{4}$ away, where the guided wavelength $\lambda_\mathrm{g} = \frac{2\pi}{\beta}$ represents the distance between two equal-phase planes along the WG. By theory, the propagation constant in a WG can be calculated via

$$\beta = \sqrt{k^2 - \left(\frac{m\pi}{a}\right)^2 - \left(\frac{n\pi}{b}\right)^2}, \tag{1}$$

where k denotes the wave number in the filling material [8]. The microstrip probe has to be placed in the obtained E-field maximum to achieve the strongest coupling between WG and microstrip line modes. Additionally, the open microstrip line geometry was adjusted to properly transform the WG mode into a quasi-transverse electromagnetic (Q-TEM) mode, the fundamental microstrip line mode. The strongest E-field components are between the microstrip and the ground plane. Therefore, a broad T-shaped microstrip was utilized as probe, so that the dynamic electromagnetic potential between probe and ground plane is at maximum. The shorted TE mode of the WG changes its phase at the probe plane according to the input phase, so that the probe element of the microstrip line is dynamically loaded and the signal is guided away from the probe. Geometry parameters of the assembly are discussed in the following section.

Due to reciprocity, the coupling behaviors between microstrip line and WG, and vice versa, are equal. However, the matching of both ports may be different.

3. SIMPLIFIED SIMULATION MODEL

Figure 1 shows the transition assembly in a cut view, where the cutting plane is placed in the center of the longer waveguide edge a. The transition consists basically of three layers. The ground layer aluminium sheet thickness is chosen as $h_\mathrm{gnd} = 2\,\mathrm{mm}$, holding a through connection for a WR 10 waveguide and a WR 10 flange assembly surrounding it. The settings of the waveguide flanges were chosen according to [11]. The high-frequency substrate is mounted on the aluminium layer for increased stability of the thin high-frequency substrate. RO3003 material from Rogers Corp. was used with a given relative permittivity of $\varepsilon_r = 3.0$ and a dissipation factor of $\tan\delta = 0.001$ at 10 GHz [12]. Investigations of the RO3003 substrate with a simple microstrip line filter showed a dissipation factor of $\tan\delta = 0.008$ and a relative dielectric constant of $\varepsilon_\mathrm{r} = 2.97$ at lower W-band frequencies. The obtained measured substrate properties were utilized for all simulations in CST Microwave Studio [13]. The substrate thickness of 127 µm leads to a microstrip line width of $w_{50} \approx 0.3\,\mathrm{mm}$ to reach a line impedance of 50 Ω. An

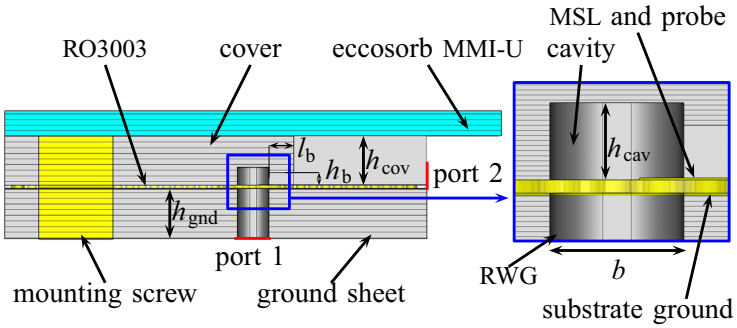

Figure 1. y-z-plane cut of the transition in side view.

aluminium cover with a milled WR 10 cavity is placed upon the microwave substrate. All WG throughs and cavities were milled with a 1 mm milling tool. Several investigations of the resulting corner radii of 0.5 mm have shown that its effect on the WG propagation behavior is negligible. Nevertheless, the fabricated WG dimensions were considered correctly in the simulation models.

The darker grey shadings in Fig. 1 represent the WG radii from the milling process. This cut view shows degrees of freedom in the cavity height h_{cav} and the height h_{b} and length l_{b} of the bounded microstrip line. l_{b} has no direct influence on the transmission behavior and was, therefore, chosen as 1 mm. The optimum cavity height $h_{\mathrm{cav}} = \frac{\lambda_{\mathrm{g}}}{4} = 1.39\,\mathrm{mm}$ at 80 GHz is calculated with Eq. (1), but the calculation of λ_{g} is based on a WG with homogeneous material filling, which is actually not the case in the proposed design. Between the cover and the aluminium ground plate, the WG is fed through the RO3003 substrate. The footprint of the WG on the substrate is cleared from copper and surrounded by VIAs to achieve the smallest field disturbances of the fundamental mode, but nevertheless the dielectric material shortens the effective guided wavelength. Hence, h_{cav} is used as optimization parameter together with h_{b}, which influences the behavior of the microstrip line directly attached to the probe. Further optimization parameters are shown in the top view of the transition, see Fig. 2. The lengths $l_{\mathrm{p}} = 0.20\,\mathrm{mm}$ and $l_{\mathrm{f}} = 0.22\,\mathrm{mm}$, as well as the width $w_{\mathrm{p}} = 0.91\,\mathrm{mm}$ of the T-shaped probe and the previously mentioned heights $h_{\mathrm{cav}} = 0.73\,\mathrm{mm}$ and $h_{\mathrm{b}} = 0.52\,\mathrm{mm}$ were optimized in CST Microwave Studio to realize the best matching at both ports and the highest forward transmission between the ports. The width and length of the bounded microstrip segment (i.e., microstrip line part from probe towards the $+y$-direction) were chosen to 0.85 mm and 1.0 mm, respectively, in order to obtain lowest

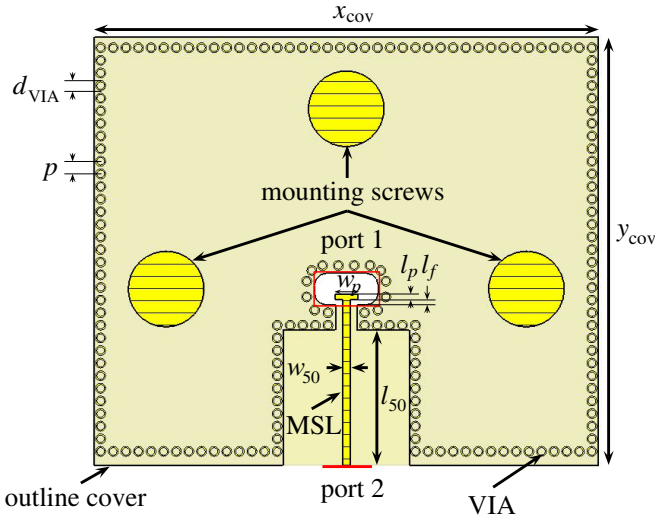

Figure 2. x-y-plane cut of the transition in top view.

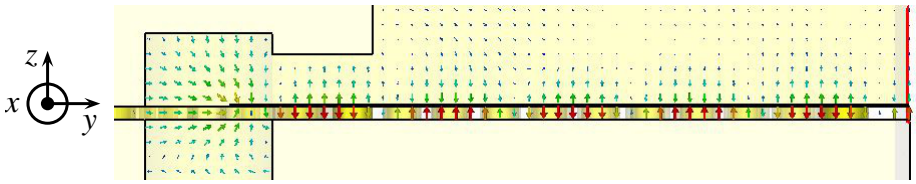

Figure 3. *E*-field distribution in the *y*-*z*-plane cut.

radiation from the transition and simultaneously not influencing the 50 Ω impedance of the microstrip line. A vector plot of the coupling *E*-field in the *y*-*z*-plane is visualized in Fig. 3. The wave is excited at port 1 which is directly attached to the WG. The *E*-field maximum at the altitude of the substrate leads to the strong *E*-field coupling to the probe element. The strong *E*-field between microstrip and ground plane indicates a very good coupling of the fundamental WG mode to the Q-TEM microstrip mode.

The used VIAs are drilled with a diameter of $d_{\mathrm{VIA}} = 0.4\,\mathrm{mm}$ and get afterwards copper galvanized until an additional copper thickness of 10 µm is reached. The VIA distance p (i.e., the distance between the center points of two neighboring VIAs) is chosen as $p = 0.5\,\mathrm{mm}$. Around the WG, a slightly larger separation of about 0.6 mm is utilized leading to a better stability of the substrate. At the WG feed-through, both copper claddings are removed, so that only the ceramic-filled PTFE substrate material with its thickness of 127 µm is left after the copper clearing, which is very unstable. With a broader strip between the VIA holes, an undesired detachment is avoided during the fabrication process.

The first planar WG port is attached to the transversal WG plane at the bottom of the ground sheet. The second port connects the microstrip line at a distance of $l_{50} = 6.5\,\mathrm{mm}$. The simulated scattering parameters are printed in Fig. 4(a). The transmission of approximately −0.8 dB is mainly driven by the losses from the microstrip line which are at a level of approx. $0.9\,\frac{\mathrm{dB}}{\mathrm{cm}}$ at 75 GHz and $1.0\,\frac{\mathrm{dB}}{\mathrm{cm}}$ at 90 GHz, so that the losses from the transition can be estimated to approx. 0.2 dB. The matching is at a very good level for both ports resulting in reflections smaller than −23 dB up to 90 GHz. Up to 100 GHz, the transition still works very well, and the reflection coefficients are smaller than −15 dB. Since the reflection coefficient worsens up to −7 dB, a utilization of the transition to 110 GHz cannot

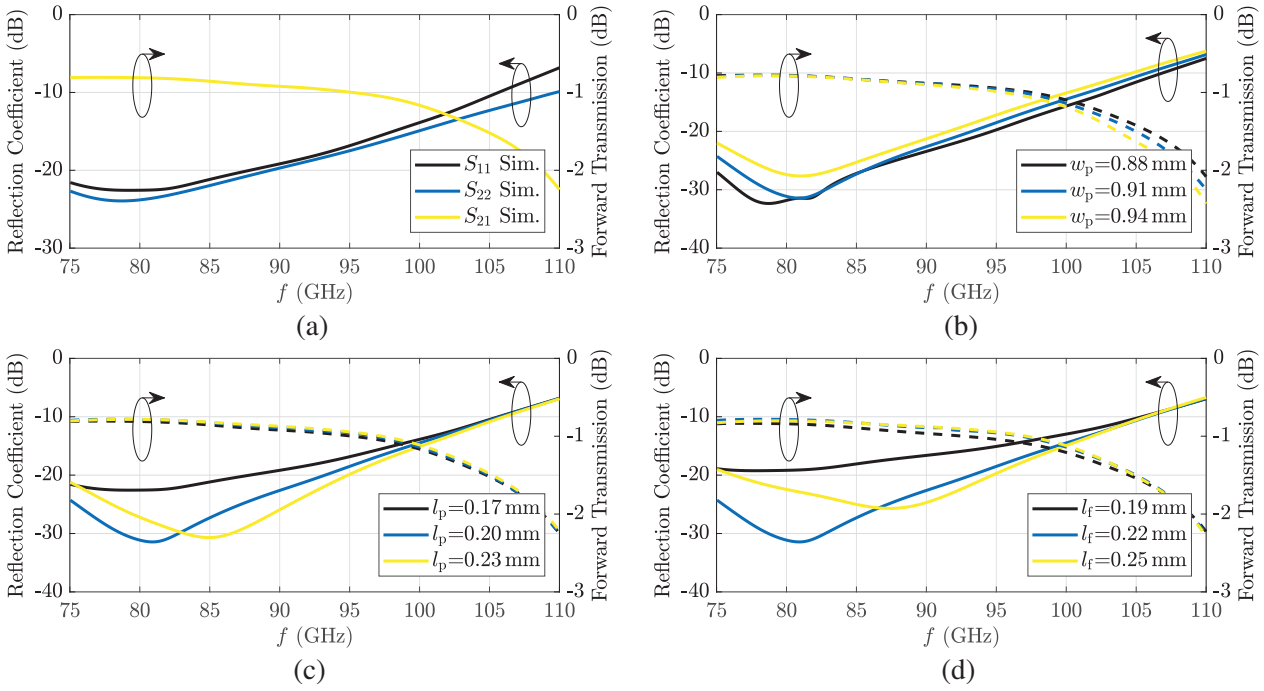

Figure 4. Simulated scattering parameters of the model shown in Fig. 2. (a) Input reflection coefficients and forward transmission coefficient. (b)–(d) Parametric study of main design parameters w_{p}, l_{p} and l_{f}. The solid lines show the reflection coefficient of port 1.

be recommended with these design parameters.

Figures 4(b)–(d) show parametric studies of the most important design parameters w_p, l_p and l_f. The transition is very robust for deviations of 30 µm, which is a common error level in substrate fabrication. The transmission is enhanced for frequencies above 100 GHz when the probe width w_p decreases.

4. MEASUREMENT MODEL AND RESULTS

The simulated model, consisting of a WG, a T-shaped probe and an microstrip line, was not convenient for measurements. Therefore, a measurement network composed of two transitions and a 180° microstrip line bend connecting them was measured with an HP 8510C vector network analyzer with external mixer modules and WR 10 WG ports. The prototype, shown in Fig. 5(a), was utilized to measure both losses from the transitions and from the microstrip line. The microstrip line is straight until the end of the cover, where it connects to a semicircle with a radius of 10 mm. The radius was obtained by the half flange diameter of the WR 10 waveguide to connect directly to the second transition and its straight microstrip line. The upper part of the picture shows the cover with the WR 10 flange and its threads and fitting holes. The high-frequency substrate is laser-structured with an LPKF Protolaser S [14]. The top-side copper cladding was not cleared where the cover lies on the substrate, as can be seen in Fig. 2.

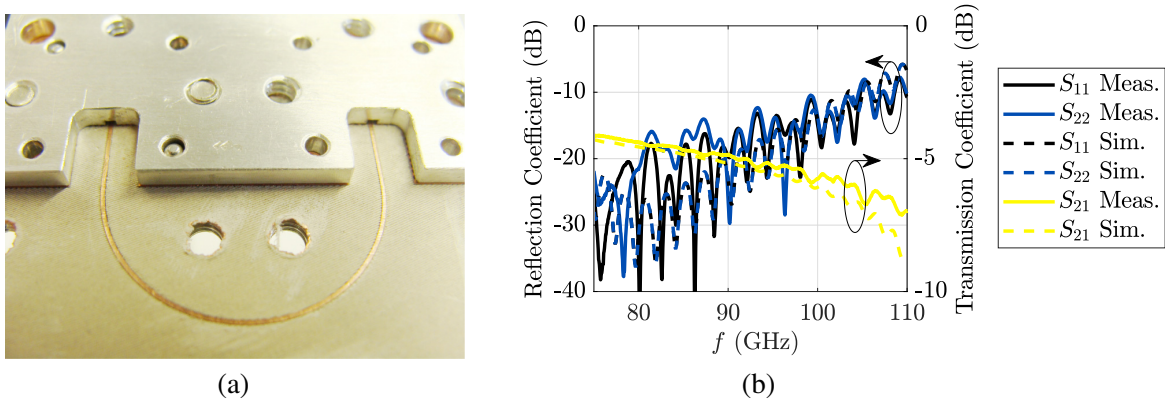

(a) (b)

Figure 5. Fabricated prototype with two transitions and a connecting 50 Ω microstrip line in (a) and corresponding simulated and measured scattering parameters in (b).

The measured scattering parameters are depicted in Fig. 5(b). The symmetric geometry predicts a symmetrical scattering parameter behavior. The simulated scattering parameters show a symmetrical behavior with reflections smaller than −20 dB over the frequency range from 75 GHz to 90 GHz and −15 dB up to 100 GHz. Translations or rotations within the assembly of back plate, substrate and back-ended stub cover, which are aligned by the register pins of the WR 10 flanges, cause asymmetries in the measurement. Nevertheless, a very low reflection coefficient of better than −14 dB is achieved for both ports in the range from 75 GHz to 90 GHz, and better than −10 dB up to 100 GHz. The ripples in the reflection coefficient curves are caused by a standing wave on the microstrip line between the transitions. The transmission between the two WG ports is at a level of −4.2 dB at 75 GHz and −4.8 dB at 90 GHz for an microstrip line length of 45 mm. Measurements of different microstrip line lengths were utilized to calculate the line loss per centimeter which was found to be approx. 0.9 $\frac{\mathrm{dB}}{\mathrm{cm}}$ at 75 GHz and 1.0 $\frac{\mathrm{dB}}{\mathrm{cm}}$ at 90 GHz for the laser-etching fabrication technique. The microstrip line losses are approx. 4.0 dB at 75 GHz and 4.4 dB at 90 GHz. Thus, the loss of a single transition is approx. 0.2 dB from 75 GHz to 90 GHz, which is at the same good value as the simulated value of approx. 0.2 dB. The finline approach in [2] is preferably used from 90 GHz to 99 GHz and shows an insertion loss of approx. 1 dB, whereas the loss of our proposed transition is only 0.2 dB. Deguchi obtained losses of approx. 0.3 dB at 76.5 GHz for his single WR 12 transition in [4] which are comparable to our design for the WR 10 waveguide.

5. CONCLUSION

A back-ended stub based WR 10 to microstrip line transition was presented. The rectangular hollow waveguide (WG) stub length and other geometry parameters of the transition have been optimized with respect to a very low reflection at both transitions, WG to microstrip line, and back to WG. The optimization was performed with a simplified simulation model. The prototype for WG based measurements consists of two transitions and a 180° microstrip line bend. The proposed WG to microstrip transition is characterized by high transmission and very low port reflectivity.

REFERENCES

1. Electronic Communications Committee (ECC), within the European Conference of Postal and Telecommunications Administration (CEPT), "ECC Recommendation (09)01: Use of the 57–64 GHz frequency band for point-to-point fixed wireless systems," Jan. 2009, [Online], Available: http://www.erodocdb.dk/docs/doc98/official/pdf/Rec0901.pdf.
2. Sun, J., F.-G. Liang, L.-H. Han, X.-Y. Sun, and Y.-Q. Zheng, "Waveguide-to-microstrip antipodal finline transition at W band," *3rd Intern. Conf. on Instrumentation, Measurement, Computer, Communication and Control*, 510–513, Sep. 2013.
3. Grabherr, W., W. G. B. Huder, and W. Menzel, "Microstrip to waveguide transition compatible with mm-wave integrated circuits," *IEEE Trans. Microw. Theory Techn.*, Vol. 42, No. 9, 1842–1843, Sep. 1994.
4. Deguchi, Y., K. Sakakibara, N. Kikuma, and H. Hirayama, "Millimeter-wave microstrip-to-waveguide transition operating over broad frequency bandwidth," *MTT-S International Microwave Symposium Digest*, 2107–2110, Jun. 2005.
5. Brazález, A. A., E. Rajo-Iglesias, J. L. Vázquez-Roy, A. Vosoogh, and P. S. Kildal, "Design and validation of microstrip gap waveguides and their transitions to rectangular waveguide, for millimeter-wave applications," *IEEE Trans. Microw. Theory Techn.*, Vol. 63, No. 12, 4035–4050, Dec. 2015.
6. Seo, K., "Planar microstrip-to-waveguide transition in millimeter-wave band," *Advancement in Microstrip Antennas with Recent Applications*, INTECH Open Access Publisher, 2013.
7. Seo, K., A. Nakatsu, K. Sakakibara, and N. Kikuma, "Via-hole-less planar microstrip-to-waveguide transition in millimeter-wave band," *China-Japan Joint Microw. Conf.*, 1–4, Apr. 2011.
8. Pozar, D. M., *Microwave Engineering*, 4th Edition, John Wiley & Sons, New Jersey, 2012.
9. Spinner GmbH, "TD-00036, cross reference for hollow metallic waveguides," Munich, Germany, 2017, [Online], Available: http://www.spinner- group.com/images/download/technical documents/SPINNER TD00036.pdf.
10. Hamberger, G. F., S. Trummer, U. Siart, and T. F. Eibert, "A single layer dual linearly polarized microstrip patch antenna array for automotive applications in the 77 GHz band," *IEEE Intern. Symp. on Phased Array Systems and Techn.*, 1–4, Oct. 2016.
11. Spinner GmbH, "TD-00077, anges for ordinary rectangular waveguides," Munich, Germany, 2017, [Online], Available: http://www.spinner- group.com/images/download/technical documents/SPINNER TD00077.pdf.
12. Rogers, "RO3000 series circuit materials," 2017, [Online], Avail- able: www.rogerscorp.com/documents/722/acs/RO3000-Laminate-Data-Sheet-RO3003-RO3006-RO3010.pdf/.
13. CST Computer Simulation Technology, "Microwave Studio," Darmstadt, Germany, 2017, [Online], Available: http//www.cst.com.
14. LPKF, "Technische Daten: LPKF Protolaser S," Garbsen, Germany, 2017, [Online], Available: www.lpkf.de/produkte/rapid-pcb-prototyping/laserstrukturierung/laser-strukturieren-leiterplatten-prototypen-kleinserien.htm.